Proceedings World Geothermal Congress 2015
Melbourne, Australia, 19-25 April 2015

Dynamic Simulation of a Supercritical ORC using Low-Temperature Geothermal Heat

Christian Vetter, Hans-Joachim Wiemer

Karlsruhe Institute of Technology, Hermann-von-Helmholtz-Platz 1, 76344 Eggenstein-Leopoldshafen

c.vetter@kit.edu, wiemer@kit.edu

Keywords: Binary cycle, ORC, supercritical, part load, dynamic simulation, control

ABSTRACT

Low temperature heat between 100°C – 160°C can be used for power production via Organic Rankine Cycles (ORC). In order to study the optimization possibilities of ORC processes, the test facility MoNiKa (Modular low-temperature cycle Karlsruhe) is being built at the Karlsruhe Institute of Technology (KIT). It is designed as a small and compact power plant with a thermal power of 1000 kW. The modular structure enables the use and investigation of different components. The geothermal heat source is realized by a conventionally heated water cycle at the site of KIT. Previous investigations showed that supercritical cycles achieved a rise of the net power output up to 44% compared to sub-critical cycles with isopentane, as they enable better adaptation of the temperature profiles in the heat exchanger. The planned test system is therefore designed for a supercritical process with propane as working fluid with live steam parameters of 5.5 MPa and 117 °C. This contribution contains dynamic simulation results of this new ORC at different load cases. In particular, a detailed analysis of the cooling of the cycle at varying cooling air conditions as well as a comparison of different control strategies concerning the achievable net power in part-load operation are presented. The results showed that the air temperature has great influence on the power requirements of the cooler which leads to a power consumption up to one-third of the produced electricity at high ambient temperatures. This problem can be countered by cooling the air by injecting fine water in so called hybrid mode and by an adaption of the desired condensation temperature to the outdoor temperature. The results of the part load simulations illustrate the optimization potential due to the use of appropriate control strategies. While at fixed pressure operation and constant turbine speed, a continuous decrease in the specific net power is inevitable, a constant specific net power can be achieved over a wide load range by using a turbine with variable speed and a frequency converter. Alternatively, a comparably good part load behavior can be realized by adjusting the live steam temperature to the load via a function developed in this study. This detailed analysis of the plant behavior allows for a more accurate prediction of the electricity production to be expected. In addition, requirements for the components to be applied can be derived from the simulation results.

1. INTRODUCTION

In addition to hydropower, wind and solar energy, geothermal energy offers another possibility of power production at low-CO_2 emissions. Geothermal brines, for example, are often available at temperatures below 160C for energy production. In the range of 100-160°C power production can be realized by transferring the heat to a binary cycle. Most of these binary cycles are realized via Organic Rankine Cycles (ORC), which operate in contrast to conventional steam processes with organic working fluids. In future it should also be possible to open up sites without aquifers for geothermal use. In this case a fracture system has to be generated in which injected water can circulate and be heated up by the hot rock. This technique is also referred to as Enhanced Geothermal System (EGS) and is currently still in the research stage. In 2009, geothermal power plants with a capacity of 10.7 GW_{el} were installed worldwide [IEA (2011)]. Most of them are installed at so-called high-enthalpy sites with temperatures exceeding 200°C along plate boundaries and tectonic upheavals such as the Pacific Ring of Fire or Iceland. At these locations one can find a significantly higher geothermal gradient, so that high temperatures at relatively low drilling depths can be obtained. Only 11% of the installed power is generated via binary cycles, however, within the geothermal power generation they have the highest growth rate [IEA (2011)]. In a future scenario of the International Energy Agency (IEA), the increase in geothermal electricity production up to 200 GW_{el} by 2050 is considered possible [IEA (2011)]. Over half of the installed capacity might then be provided by the use of low temperature heat sources and EGS, where also binary circuits will be used. This shows a great potential for Organic Rankine Cycles in future applications.

At the development and design stage of ORC power plants, a variety of boundary conditions have to be taken into account concerning the optimal system design. Besides the temperature level and the available heat, the type of use in the overall concept (combined heat and power generation, grid connection or island operation ...) must be considered. With the goal to open up potentials for a more efficient power production from low-enthalpy heat the test facility MoNiKa (Modular low temperature cycle Karlsruhe) is being built at the campus of the KIT. Previous studies [Vetter et al. (2013)] showed that significant performance improvements are possible through an operation at supercritical pressures. Therefore, in MoNiKa a supercritical ORC is to be realized. The modular approach of the facility is intended to enable the use of various heat exchangers, turbines and pumps, so that the individual power plant components can be characterized over a wide operating range. Since there is no geothermal well at the campus of the KIT, an artificially produced thermal water circuit is used, which is heated by an oil burner. The power plant is being built into standard shipping containers, so that a future mobile use on real geothermal sites is possible. For the design of the ORC process the following boundary conditions were defined:

- Temperature of geothermal fluid at entry of heat exchanger: 150°C
- Thermal power at full load: 1000 kW
- Condensation temperature: 30°C

In the scope of this contribution a detailed process analysis is presented. This includes the study of partial load behavior of individual components as well as of the entire process when varying the geothermal fluid mass flow and the cooling air condition.

In addition, different control strategies are presented and compared taking into account the dynamic system behavior. This allows the calculation of various diurnal variations with and without heat extraction.

2. MODELLING

2.1 Thermodynamics of Organic Rankine Cycles

The Clausius-Rankine cycle with water as the working fluid is state of the art in coal and nuclear power plants [Tchanche et al. (2011)]. Due to the low temperatures this process is not suitable for geothermal electricity generation. Therefore in a so called Organic Rankine Cycle (ORC) organic fluids are used instead of water as working medium. These are characterized in comparison to water by lower evaporation temperatures and pressures. The changes of state of the working fluid in the cycle are the same as in the water-steam cycle. In the ideal case, these are:

- 1 - 2: Isentropic compression in the pump
- 2 - 3: Isobaric heating in the heat exchanger
- 3 - 4: Isentropic expansion in the turbine
- 4 - 1: Isobaric cooling in the condenser

The above-mentioned ideal state changes of the working fluid cannot be achieved in reality. In the heat exchanger and condenser pressure losses cannot be avoided. Due to friction and turbulence, an increase in entropy within the pump and the turbine occurs. This deviation from the ideal state changes is usually defined via the isentropic turbine and pump efficiency $\eta_{Turbine}$ and η_{Pump}:

$$\eta_{is,Turbine} = \frac{h_3 - h_4}{h_3 - h_{4,is}} \tag{1}$$

$$\eta_{is,Pump} = \frac{h_{2is} - h_1}{h_2 - h_1} \tag{2}$$

where h are the specific enthalpies at the different states of the process, which are indicated with index numbers according to figure 1. The index *is* signifies the isentropic change in state. The gross power is than calculated with the specific enthalpies at inlet and outlet of the turbine and with the ORC mass flow:

$$P_{gross} = \dot{m}_{ORC}\left(h_3 - h_4\right) \tag{3}$$

The net power is given by the gross power minus the power requirements of the pump and further auxiliaries. The pump power can also be calculated via the specific enthalpies, the biggest part of the auxiliaries' power is needed for the fans of the cooler. Other system parts can therefore be neglected.

$$P_{net} = \dot{m}_{ORC}\left(h_3 - h_4 - \left(h_2 - h_1\right)\right) - P_{Fan} \tag{4}$$

Assuming an ideal insulated heat exchanger, heat losses to the environment can be neglected. The supplied heat is then identical to the heat extracted from the geothermal fluid. This heat can be calculated with the average specific isobaric heat capacity c_p, the mass flow $\dot{m}_{geo}$ and the temperatures of the geothermal fluid $T_{geo,in}$ and $T_{geo,out}$ at inlet and outlet of the heat exchanger.

$$\dot{Q}_{in} = \dot{m}_{geo}\bar{c}_p\left(T_{geo,in} - T_{geo,out}\right) = \dot{m}_{ORC}\left(h_3 - h_2\right) \tag{5}$$

For the direct comparison of the net power of different cycles a new characteristic factor has been defined: The specific net power $P_{net,spec}$ indicates the net power which can be produced by a given geothermal fluid mass flow of 1~kg/s.

$$P_{net,spec} = \frac{P_{net}}{\dot{m}_{geo}} \tag{6}$$

In previous work [Vetter et al. (2013)] stationary simulations with various workings fluids have been performed and compared to cycles with the state of the art workings fluids isobutane and isopentane with the goal to maximize the specific net power output. The investigations showed that at maximum net power supercritical processes show slightly lower thermal efficiencies compared to sub-critical processes. However, significantly higher exergetic efficiencies at the heat transfer and thus a higher heat input can be achieved, so that a performance increase by up to 44% is possible compared to a subcritical isopentane process at the same mass flow of geothermal fluid. However, the top five values of the specific net power occurred with fluids, which possess a high to very high greenhouse warming potential (GWP) with values ranging from 675 to 10300. With a GWP of 3 and lying at sixth position with a slightly lower specific net power the propane process is thus the preferable alternative. A supercritical propane process shows an improvement in the specific net power by 17% compared to isobutane and 35% compared to isopentane. The test facility is therefore being built as a supercritical propane cycle with a live steam pressure of 5.5~MPa and a live steam temperature of 117°C. The design point of the process is shown in the T-s-diagramm and in the h-s-diagram in Figure 1.

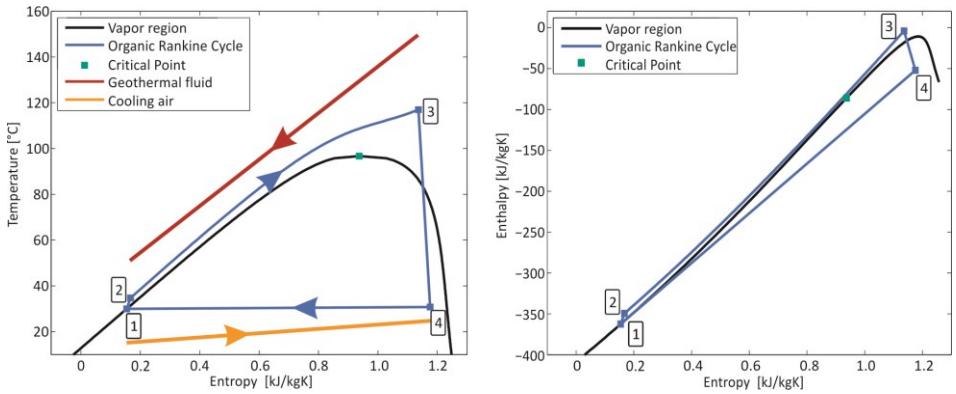

Figure 1: T-s-diagram (left side) and h-s-diagram (right side) of the design point of the simulated supercritical process, in T-s-diagram schematic illustration of the temperature curves of geothermal fluid (red) and cooling air (yellow)

2.2 Dynamic system model

Based on the thermodynamic design presented in the previous section a P&I-diagram of the test facility has been developed. A simplified version of this diagram is shown in figure 2 and served as basis for the dynamic system model. The propane cycle is shown in green and includes a feed pump, a heat exchanger, a turbine with bypass and generator, a hybrid cooler and a feed tank. The heat is supplied in the heat exchanger through the water cycle consisting of heating system and pump. In both cycles, the fluid conditions of the design case are shown at characteristic points.

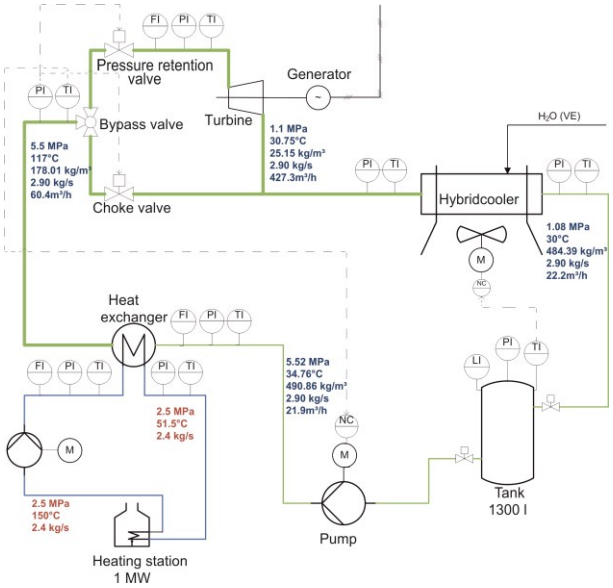

Figure 2: Simplified P&I-Diagram of the simulated system consisting of the geothermal fluid loop (blue) and the ORC (green) with pump, heat exchanger, turbine, hybrid cooler and tank

The transient model has been built in the simulation environment Dymola [Dymola (2012)] using the commercial Modelica library TIL [TIL (2012)] which enables the embedding of the fluid property calculation of REFPROP [NIST (2010)]. In all components the conservation laws of mass, energy and momentum are implemented in the following form:

$$\frac{dM}{dt} = \sum \dot{m}_k = \rho_{\text{hom}} \frac{dV}{dt} + V \frac{d\rho_{\text{hom}}}{dt} \tag{7}$$

$$\frac{dh}{dt} = \frac{1}{M}\left\{\sum\left[\dot{m}_k\left(h_k - h\right)\right] + \dot{Q} + \dot{W}_t + V\frac{dp}{dt}\right\} \tag{8}$$

$$\frac{d\dot{m}}{dt}\frac{V}{A} = \frac{\dot{m}_{in}^2}{A\rho_{\text{hom}}} - \frac{\dot{m}_{out}^2}{A\rho_{\text{hom}}} + \left(p_{in} - p_{out}\right)A - \Delta p_{fr} \tag{9}$$

where M is the mass of the control volume V, $\dot{m}_k$ are the mass flows entering and leaving the volume, ρ_{hom} is the homogenous density of the fluid, h_k are the specific enthalpies of the fluids, h is the enthalpy of the control volume, $\dot{Q}$ are the heat flows, $\dot{W}_t$ is the shaft work, A is the cross-sectional area and Δp_{fr} is the friction pressure loss. Differences in height are neglected as well as fast dynamic processes, which results in a quasi-stationary momentum balance since the time derivative of the momentum is set to zero. The friction pressure loss is significantly higher than the pressure changes due to density changes; therefore the change of the momentum flows can also be neglected.

To build up the dynamic model the main components had to be characterized in more detail. This included the dimensioning of the heat exchanger and the hybrid cooler and is presented in the following sections.

2.2.1 Feed pump and cooling fans

The feed pump is modelled as a 0-dimensional component with constant isentropic efficiency of 70%. The power consumption of the pump is calculated as follows:

$$P_{hyd} = \Delta p \cdot \dot{V} \tag{10}$$

$$P_{Pump} = \frac{1}{\eta_{is,Pump}} P_{hyd} \tag{11}$$

where P_{hyd} is the hydraulic power added to the fluid and P_{Pump} is the power consumption of the pump motor.

The required power of the fans of the hybrid cooler is calculated in the same way with the volume flow of air and the pressure loss of the air side of the hybrid cooler. The fans are modeled with a constant efficiency of 70%.

2.2.2 Turbine

For the modelling of the turbine a 0-dimensional turbine model is used which calculates the expansion of the steam as a function of displacement volume dV, speed n and isentropic efficiency of the turbine. The produced power is:

$$P_{turb} = \dot{m}_{ORC}\left(h_3 - h_{4is}\right) \cdot \eta_{turb,is} \tag{12}$$

The mass flow is connected with the density ρ_3 at turbine entry via:

$$\dot{m}_{ORC} = \rho_3 \cdot n \cdot dV \tag{13}$$

For more detailed calculations of the part load behavior, the model was extended with a variable load-dependent isentropic efficiency. An adaption of the efficiency used by Ghasemi et al. (2013) was implemented so that deviations of the volume flow and the enthalpy drop in comparison to the design point (index DP) were taken into account. The adaption is realized via the following equations:

$$r_{h1} = \sqrt{\frac{h_3 - h_4}{\left(h_3 - h_4\right)_{DP}}} \tag{14}$$

$$r_h = \left(\left(\left(1{,}389 \cdot r_{h1} - 5{,}425\right) \cdot r_{h1} + 6{,}274\right) \cdot r_{h1} - 1{,}866\right) + 0{,}619 \tag{15}$$

$$r_{V1} = \sqrt{\frac{\dot{V}}{\dot{V}_{DP}}} \tag{16}$$

$$r_V = \left(\left(\left(-0{,}21 \cdot r_{V1} + 1{,}117\right) \cdot r_{V1} - 2{,}533\right) \cdot r_{V1} + 2{,}588\right) + 0{,}038 \tag{17}$$

$$\eta_{is} = \eta_{is,DP} \cdot r_h \cdot r_V \tag{18}$$

2.2.3 Heat Exchanger

The heat exchanger is modelled as a counter flow plate heat exchanger and is discretized in flow direction with 50 cells. In each cell the transferred heat Q is calculated as a function of the heat transfer area A_{HT}, the mean temperature difference and the heat transfer coefficient k:

$$\dot{Q} = k \cdot A_{HT} \cdot \Delta \upsilon_{\ln} \tag{19}$$

The logarithmic mean temperature difference is calculated as a function of the temperature differences at entry and exit of the cell:

$$\Delta\upsilon_{\ln} = \frac{\Delta\upsilon_1 - \Delta\upsilon_2}{\ln\left(\frac{\Delta\upsilon_1}{\Delta\upsilon_2}\right)} \tag{20}$$

The heat transfer coefficient is calculated as follows:

$$\frac{1}{k} = \frac{1}{\alpha_{ORC}} + \frac{b_P}{\lambda_P} + \frac{1}{\alpha_{geo}} \tag{21}$$

where α_{ORC} and α_{geo} are the convective heat transfer coefficients of the ORC fluid and the geothermal fluid, b_P is the thickness of the heat exchanger plates and λ_P is the heat conductivity of the plate material. The heat transfer coefficients are calculated via a Nusselt-number correlation for plate heat exchangers (for detailed information see [Martin (2010)]).

2.2.4 Hybrid Cooler

The hybrid cooler is modeled as a cross-flow heat exchanger with plate fins to enhance the heat transfer area on the air side. It is discretized in flow direction with 20 cells. The condensation of the ORC fluid takes place inside of the horizontal arranged pipes. For the calculation of the heat transfer equation 19 and 20 are used, the heat transfer coefficient is calculated as follows:

$$\frac{1}{k} = \frac{1}{\alpha_{air}} + \frac{A_{out}}{A_{in}}\left(\frac{1}{\alpha_{in}} + \frac{d_{out} - d_{in}}{2\lambda}\right) \tag{22}$$

where α_{air} is the convective heat transfer coefficient on the air side, α_{in} is the convective heat transfer coefficient inside the pipes, A_{out} and A_{in} are the heat transfer surfaces inside and outside the pipes and d_{out} and d_{in} are the outer and inner diameter of the pipes. The heat conductivity of the pipe material is described by λ. The heat conduction coefficient on the air side is calculated by using a correlation by von Haaf [von Haaf (1988)], the heat conduction coefficient of the ORC side is calculated via a Nusselt-number correlation for condensation inside horizontal pipes [Numrich and Müller (2010)].

The pressure loss of the air side which is needed for the calculation of the fan power is given by

$$\Delta p = \xi \frac{u}{d_e}\frac{\rho}{2} w^2 \tag{23}$$

where u is the distance of the pipe rows, w the velocity of the air flow and d_e an equivalent diameter of the pipes, which is influenced by the geometry of the fins (for more information see [von Haaf (1988)]). The friction factor ξ is calculated in accordance to the Reynolds-number Re as follows:

$$\xi = 10{,}5 \cdot \mathrm{Re}^{-1/3}\left(\frac{d_e}{u}\right)^{0{,}6} \tag{24}$$

In hybrid mode it is possible to cool down the air flow by adding a fine spray of water which dissolves in the air. This reduces the temperature of the air, since the energy required to evaporate the water, is removed from it. At the same time the relative humidity of the air rises. The temperature which is reached at saturation is called cooling limit temperature. Cooling down to temperatures below this temperature is not possible. The calculation of this change of state which is assumed to be isobaric can be carried out via a mass and energy balance. Therefore the air is treated as a mixture of the ideal gases dry air and water steam.

3 DYNAMIC SIMULATION

The boundary conditions which influence the net power output are the temperature of the cooling air and the mass flow of the geothermal fluid. Therefore, on the one hand the control of the hybrid cooler at full load and variable inlet conditions of the cooling air has been investigated; on the other hand the dynamic part load behavior at decreased mass flow of the geothermal fluid has been calculated. Finally, based on climate data typical for central Europe exemplary diurnal variations of cooling air condition were defined in order to obtain a realistic statement of the seasonally dependent power production with and without heat extraction.

3.1 Influence of cooling air condition

To investigate the influence of the inlet condition of the cooling air to the process simulations were carried out at full load with varying temperature and varying relative humidity of the cooling air. For the calculations the mass flow of geothermal fluid, the condensation temperature and the live steam condition were kept constant, the mass flow of the cooling air and the mass flow in the ORC have been adapted by a PI controller. The temperature of the cooling air was varied within the range of 0 °C to 40 °C, the relative humidity from 0% to 80%. In a first step the simulations have been carried out without water injection (dry mode). Under this condition the relative humidity has negligible influence on the process. A variation of the ambient temperature showed a high power requirement of the fans with rising temperatures. In figure 3 the resulting specific net power according to varying ambient temperatures is shown (blue line). At a cooling air temperature of 0 °C the specific net power is 41,5 kWs/kg, but it decreases up to a value of 10,7 kWs/kg at 40 °C cooling air temperature. In the range from 0 °C to 15 °C there is only a small dependency, while

starting from a cooling temperature of 15 °C the specific net power decreases progressively. For cooling air temperatures higher than 20 °C simulations resulted in a linear decrease of the specific net power. These characteristics can be explained by the power consumption of the cooling fans which is also shown in figure 3 (red line). The power consumption rises progressively up to an ambient air temperature of around 19 °C when the fans provide the maximum possible mass flow. At higher temperatures the fan power changes only due to temperature dependent changes of the air properties. This means that in the range from 19 °C on the cooling air mass flow can´t take the heat which has to be removed during condensation. This results in a change of the condensation temperature and pressure, which in the end results in a smaller usable enthalpy drop in the turbine and therefor in a reduced gross power.

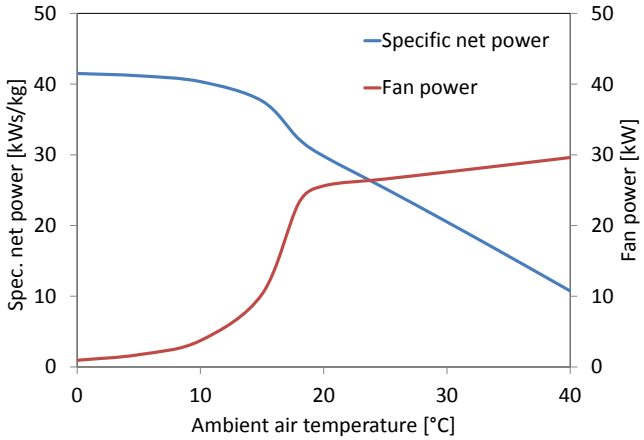

Figure 3: Specific net power and required fan power at full load according to different ambient air temperatures

The strong performance decrease of the specific net power at cooling air temperatures higher than 20 °C shows that activities to improve the cooling are reasonable. An increase of the provided maximum air mass flow would enable a constant condensing temperature and gross power, however, it would also lead to an even greater increase in the power consumption of the fans. Alternatively, cooling the air by adding fine water spray in the so called hybrid mode offers a good possibility. Figure 4 shows a comparison between the specific net power in dry and in hybrid mode. In hybrid mode water is injected at ambient temperatures above 18 °C. The mass flow of injected water is calculated according to the ambient temperature and humidity to cool down the air flow to 18 °C or if this is not possible to the cooling limit temperature. Figure 4 shows the curves of the specific net power as a function of ambient temperature of the cooling air at a relative humidity of 0% and 60%. For comparison, the curve of the specific net power without water injection known from Figure 3 is plotted. Below the air temperature of 18°C, the curves are identical, since no water is injected. In dry air (phi = 0%) the desired temperature of 18 °C can be maintained in the considered range up to 40 °C by injecting water. At 40 °C inlet temperature, the addition of the cooling water leads to a relative humidity of the air of 69.9%, maintaining the desired temperature of 18°C would thus be possible for even higher temperatures. In this case, the specific net power can be kept constant at the value which is achieved at an air temperature of 18 °C, because the rising air humidity as described above has a very small influence on the power requirement of the fans. At an air temperature of 30 °C, for example, the specific net power can be increased from 20.5 kWs/kg to 32.3 kWs/kg, which corresponds to an increase of 57%. The required water consumption is then 0.58 kg/s. However, dry air at a relative humidity of 0% represents only a theoretical case in most climates. Therefore, in Figure 4 also the specific net power is shown at an air humidity of 60%. At this relative humidity, the target temperature can be maintained up to an inlet temperature of 22.7 °C. For higher temperatures the cooling air is cooled down to the respective cooling limit temperature. This leads to a decrease of the specific net power as in dry mode, however, the curve of the specific net power shifts in each case by the amount of the possible cooling to higher cooling air temperatures.

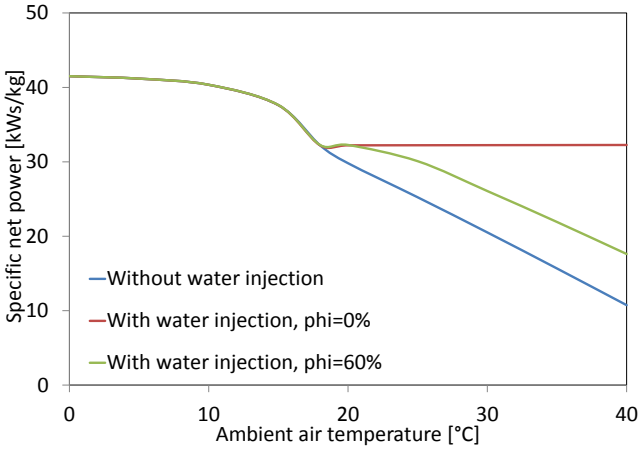

Figure 4: Specific net power at dry mode (no water injection) and hybrid mode (with water injection) for different air humidities phi at varying ambient air temperature

In this way, performance increases between 4.8 kWs/kg and 6.8 kWs/kg are possible at inlet temperatures between 25 °C and 40 °C. At an ambient temperature of 30 °C this leads to an improvement of the specific net power by 27% by the addition of 0.3 kg/s of cooling water.

In the previous simulations, the control of the air mass flow aimed to comply with the constant condensation temperature of the design point. When deviating from the design case, however, it is not guaranteed that this control leads to the highest net power. Therefore, simulations were carried out with the variation of the condensation temperature at different air temperatures. Figure 5 shows the curves of the in this way calculated specific net power at air temperatures of 0 °C, 10 °C, 15 °C and 35 °C, in accordance to the condensation temperature. Figure 5 clearly shows that to every ambient temperature a condensation temperature can be assigned where an optimum of the specific net power can be achieved. These optimum condensation temperatures are lower than the design condensation temperature of 30 °C for ambient temperatures below 15 °C, for higher cooling air temperatures an increase of the condensation temperature is of advantage. At an air temperature of 0 °C, a power increase of 18% is possible by lowering the condensation temperature from 30 °C to 15 °C. This reduces the pressure after the condenser to 8.4 bar. When lowering the condensation temperature it must therefore be noted that the turbine can handle the resulting higher pressure drop. The 0-dimensional model used in this study can't provide information about this. Only the effect of the deviation from the design point on the isentropic efficiency of the turbine is calculated. With the described model the isentropic efficiency decreases due to the pressure change, so that the higher enthalpy drop has a stronger influence and leads to an increase of the gross power of the turbine. At an air temperature of 35 °C, the condensation temperature of 30 °C can't be achieved, even with the water injection. The lowest possible condensing temperature is 39.4 °C. By increasing the condensation temperature to 45 °C the power consumption of the fans can be reduced considerably, so that an improvement in the specific net power of 18% can be achieved. Simultaneously, the required mass flow of the cooling water is reduced from 0.35 kg/s to 0.19 kg/s, although the humidification of the air is still at most, because the required cooling air mass flow decreases correspondingly. Based on the condensation temperature at which the maximum net power has been calculated, a function has been developed, which assigns every ambient temperature an optimum condensation temperature. This makes it possible to adapt the set point of the temperature at condenser outlet, which determines the cooling power, variable to the respective air temperature. As an approximation, it is considered that the condensation temperature should be higher of about 15 °C than the ambient air temperature.

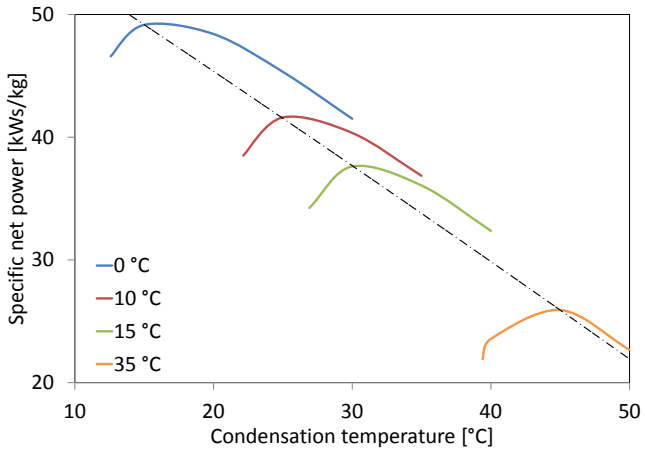

Figure 5: Specific net power at different ambient air temperatures according to condensation temperature

The analysis of the hybrid cooler showed that the cooling air temperature in particular at high ambient temperatures had a great influence on the achievable net power. However, it became clear that improvements in the power requirement of the cooler are made possible by the injection of water and by a control of the condensation temperature adapted to the ambient temperature.

3.2 Part load behavior

In the case of heat extraction parallel-connected to the power plant, the supplied geothermal fluid mass flow to the power plant is reduced. Under certain circumstances this set-up can lead to part load operation over a majority of the total operating hours depending on the heat demand. Therefore, the analysis and optimization of the power plant behavior at reduced geothermal fluid mass flow is of particular interest. In case of deviations from the design point usually the ORC - mass flow needs to be adjusted. This change in the mass flow causes a change of the pressure drop over the turbine. Live steam pressure and temperature can then be influenced only by specific control interventions. In this contribution, three different control strategies have been implemented in the model:

- Fixed pressure with variable turbine speed
- Fixed pressure with pressure retention valve
- Sliding pressure

In both control strategies with fixed pressure the pressure after the feed pump, i.e. the pressure at which the heat is supplied, is kept at a constant value. The live steam temperature is also kept at the value of the design point by adjusting the ORC mass flow with a PI controller. The two strategies differ in the control of the turbine. When using a pressure retention valve the turbine operates at a constant speed of 50 Hz. By the reduction of the mass flow at part load the pressure drop over the turbine is reduced. Since the lower pressure level of the process is defined by the condenser, this means a decrease at the turbine inlet. To keep the pressure in the heat exchanger at constant level, thus a partial expansion of the supercritical propane must be carried out by a pressure retention valve upstream of the turbine. Alternatively the speed of the turbine can be adjusted at part load to maintain the pressure drop of the

design point and therefor in this case no partial expansion is necessary. Then the pressure extension valve can be left uncontrolled fully opened. The varying speed requires the use of a frequency converter for grid connection of the plant. At the sliding pressure control, the third possible control strategy, the turbine runs with constant speed and the pressure retention valve is fully opened. In this case, the pressure in the heat exchanger results automatically from the ORC mass flow. With decreasing mass flow the pressure also decreases which leads to subcritical pressures at load cases below 66% load. To keep the live steam temperature at constant value would be possible with this control strategy but isn't useful, since it would lead to a superheating of the ORC fluid, which reduces the mass flow. Therefore a function for the live steam temperature in accordance to the geothermal mass flow has been developed to obtain live steam states which lead to an expansion to the same state as at full load. The desired temperature can be adjusted by controlling the ORC mass flow.

Figure 6 shows the resulting part load curves of the different control strategies at a reduction of the geothermal fluid mass flow up to 17% of the design point value. It can be seen that the fixed pressure control with variable speed and the sliding pressure control in the load range of 50% - 100% result in a nearly identical specific net power. Starting from 37.6 kWs/kg at full load, a slight improvement in performance to 39.6 kWs/kg can be achieved in this part-load range. This can be explained by the strongly decreasing power demand of the fans. While at fixed pressure control this stable power curve is given by the nearly constant turbine power, at sliding pressure the decreasing turbine power is compensated by the decreasing power consumption of the feed pump. At fixed pressure control with pressure retention valve the constant power requirement of the pump combined with the decreasing gross power of the turbine leads to a significantly reduced specific net power at part load. When using fixed pressure control, at 50% load an increase of the specific net power of 11.2 kWs/kg can thus be achieved by using a variable speed turbine instead of a pressure retention valve, which means an improvement of 30%. In the range below 50% load simulations showed that at sliding pressure the stronger decreasing turbine power can't be compensated anymore by the lower power requirement of the pump. The fixed pressure control with variable speed therefore has the highest specific net power when comparing the control strategies for these load cases. At 17% load, the specific net power in this case is 28.1 kWs/kg, compared to 9.4 kWs/kg at sliding pressure. At fixed pressure control with pressure retention valve the system already requires more energy than can be converted in the turbine. This results in a specific power demand of 8.2 kWs/kg.

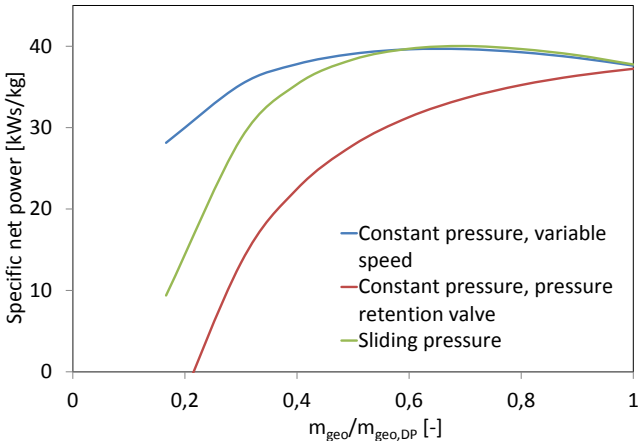

Figure 6: Comparison of the specific net power at part load with different control strategies

The comparison of the control strategies showed that with the supercritical ORC a very good partial load behavior over a wide load range is possible with appropriate control. In addition, it became clear that the choice of the control strategy has great influence on the whole process and the achievable net power. In particular, the operation at fixed pressure with variable turbine speed represents in this case an interesting alternative especially at very low load below 50%. But also the sliding pressure with appropriately adapted live steam temperature allows efficient operation up to 50% load. On the other hand, at conventional fixed pressure operation with pressure retention valve the high pressures of the supercritical process lead to a significantly worse part load behavior.

3.3 Diurnal variations

For simulating diurnal variations curves of temperature and relative humidity of the cooling air have been defined. As a basis for these curves data of the measuring station of the German Weather Service (DWD) in Rheinstetten near Karlsruhe, Germany [62, 92] from the year 2012 were used. Three different profiles were determined, corresponding to a representative winter, spring/autumn and summer day. For the seasonal-typical curves the hourly values for all days of the months of February (winter), April (spring) and August (summer) were averaged. With these three cases, the climatic conditions in Central Europe and in climatically similar sites are thus well reproduced. Simulations of the 24-hour operation of the ORC at full load have been carried out using these temperature profiles as boundary condition for the cooling air at the entry of the cooler. In figure 7 the resulting diurnal variations of the specific net power are shown. The dotted lines represent the specific net power at operation with constant set point condensation temperature of 30 °C, the continuous lines result from the before mentioned adaption of the condensation temperature to the ambient temperature. At constant condensation temperature the highest net power of around 100 kW can be achieved in winter, as in this case the power consumption of fans is at very low values of around 1 kW due to the low air temperatures. For the same reason an approximately constant power generation can be realized. In spring the power requirement of the cooling has greater influence. At night a net power output of 98 kW can be achieved, but during day time the air mass flow required for cooling the system rises with the ambient temperature and with this the power consumption of the fans. Thus, the net

power output decreases at midday to 92 kW. However, in summer the effect of the higher temperatures on the net power output is considerably higher. Here, the net power output is already in the night at a maximum of 90 kW, daytime values are in the range of 74.5 kW to 77 kW. By the water injection for lowering the cooling air temperature starting from ambient temperature above 18 °C, however, the power requirement of the fans, and thus the net power can be maintained to an approximately constant value. In particular, during the period 7h-10h and 18h-21h, the set point temperature of the cooling air of 18 °C can be maintained and therefore a constant performance can be achieved. From 10h to 18h the maximum possible amount of water is injected, but the air can't be cooled down to 18 °C which leads to a slight increase of the power consumption of the fans in this period. The condensation at the desired temperature of 30 °C can be realized at all time for these three scenarios, since the control of the fans adjusts fast enough to fluctuations in temperature and relative humidity and the maximum required air mass flow is lower than the power limit of the fans. The great influence of the cooling air condition is also evident when comparing the total electricity yield per day. This was calculated for the three scenarios by integrating the diurnal variations of the net power over time. In winter, therefore, a daily output of 2.4 MWh can be provided, while in spring with 2.3 MWh and in summer with 1.9 MWh the produced electricity is 4 - 20% lower. The required amount of injected water in the summer is on average 13.1 m^3 per day.

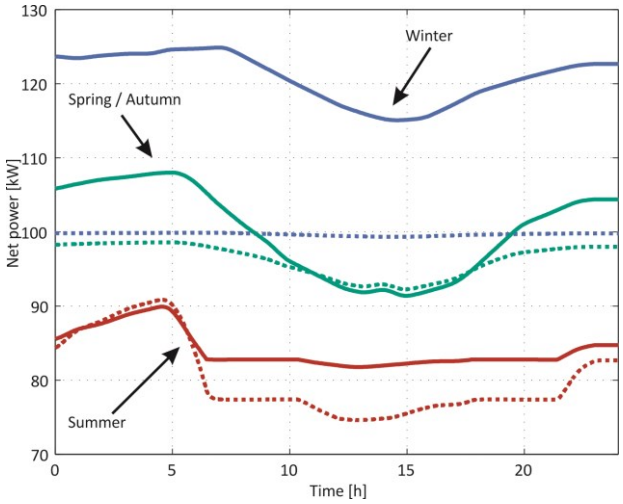

Figure 7: Diurnal variations of the net power resulting from different exemplary ambient temperature profiles; comparison of cooling control: constant condensation temperature (dotted) versus adapted condensation temperature (continuous)

In comparison to that the resulting diurnal variations of the adaption of the condensation temperature to the ambient temperature show the optimization potential by this improved control. The curve of the air temperature of the winter day leads in the case of optimized control to condensation temperatures between 14 °C and 18 °C, which allow an increase in the turbine power from 138 kW to about 169 kW. Since, in contrast, the power requirement of the cooler increases by only 6.3 kW, a higher net power by up to 25 kW can be achieved compared to a condensation temperature of 30 °C. In this way, 0.5 MWh or 21% more electricity can be produced per day. At spring and autumn days an improvement in the net power output is also possible over a wide period of time. Particularly in the period from 20h to 8h, the condensation temperature can be lowered due to the low air temperatures and thus the turbine power can be increased. The optimal condensation temperature at this time is between 21.5 °C and 23 °C. This results in an increase of the turbine power of 15 kW and of the power demand of the cooler of 7 kW, which leads to an increase in net power of 8 kW. At midday the optimum condensation temperature is of around 30°C, so that during this period no higher net power output is possible. Overall, the daily output can be increased in this way by 4% to 2.4 MWh. On summer days, the optimized cooling control leads to an opposite change in the net performance. During the night, no improvement of the power requirement of the cooler is possible; during daytime, however, a higher net power output can be achieved by a slight increase in the condensation temperature by a maximum of 2 °C. The variation of the condensation temperature in this case has only a small influence on the turbine power, which remains approximately constant. However, the power consumption of the fan decreases considerably by up to 10 kW, a decrease of 40%. As a result, during the day a higher net power by about 8 kW that can be achieved and in contrast to the control with constant condensation temperature can be kept constant even at the warmest hours at midday. Overall, this leads to an increase in daily electricity output of 5%. Moreover, the required amount of cooling water can be reduced by 17% due to the lower air mass flow rates.

In addition to the simulation of the daily curves at full load, the plant behavior of the ORC was calculated at part load. The investigated part load cases were limited here to a constant reduction of the geothermal fluid mass flow. Such reductions of geothermal fluid mass flow usually occur only at a parallel heat extraction. Based on the assumption of no heat demand in summer, the partial load diurnal variations were simulated only for the winter and spring scenario. For these cases, like at full load, the diurnal variations were calculated for a constant condensing temperature of 30 °C and with an adapted condensation temperature according to the ambient temperature. In addition, the previously mentioned different turbine and pressure control strategies have been compared. Figure 8 shows an example of the diurnal variations of the net power at a reduction of the geothermal fluid mass flow rate to 60% for the averaged spring (left) and winter day (right). It is clear that both in spring as well as in winter at sliding pressure and at fixed pressure control with variable speed a nearly constant net power of approximately 59 kW can be achieved when the condensation temperature is kept constant at 30 °C. These control strategies show a load behavior directly proportional to the geothermal fluid mass flow rate, which could be expected because of the constant specific net power in this load range. The net power at fixed pressure control and with pressure retention valve on the other hand delivers values of 46 kW – 47 kW that are significantly lower. The daily electricity output is for both scenarios at 1.4 MWh (sliding pressure, fixed pressure with variable speed) or 1.1 MWh (fixed pressure with pressure retention valve). Contrary to the full-load case approximately the same net power

can be achieved on spring days as on winter days. This can be explained by the non-linear power requirement of the fans, which is therefor at part-load only slightly higher in spring than in winter.

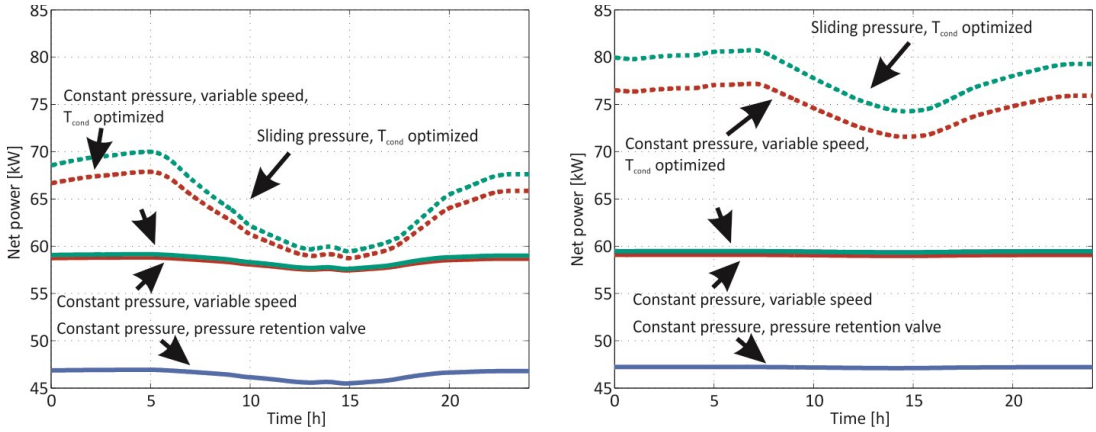

Figure 8: Diurnal variations of the net power resulting from different exemplary ambient temperature profiles at 60% load; comparison of different control strategies in spring (left side) and winter (right side)

Figure 8 also shows the diurnal variations of the net power with optimized cooling control for the sliding pressure and the fixed pressure control with variable speed by dashed lines. In the scenario of a spring day, similarly to full load, especially during the night hours a significant improvement in the net power up to 11 kW can be achieved. Contrary to the full load, also during daytime a small increase in net power of 1-2 kW is possible. Overall, the optimization has a higher influence at part load, the daily electricity production can be increased by a variable condensing temperature by up to 10% (at full load by 4%). On winter days, an increase in the net power of 18-21 kW is detected, which corresponds to an increase in performance by up to 24%, which is also slightly higher than at full load. In both scenarios, it is noticeable that at variable condensing temperature, the increase in the net power in sliding pressure will be higher than with fixed pressure. Especially on winter days at sliding pressure thus a higher net power of 3-4 kW can be achieved. The reason for this can be found in the different adjustments of the control strategies on the deviation from the design point. The lowering of the condensation temperature leads to a lower inlet temperature to the heat exchanger. By this, more heat is required to achieve the desired steam state. This causes a reduction of the ORC mass flow. In the case of fixed pressure control with variable turbine speed, this has only a minor impact on the rotation speed, while the steam state is kept constant. At sliding pressure the variation of the ORC mass flow leads to a deviating steam pressure. Since the set point temperature is determined directly from the geothermal fluid mass flow, the live steam condition changes. Thus, the increase in the enthalpy drop in the turbine is more pronounced at this control strategy than in the fixed pressure control regime.

The daily curves at part load clearly show the great influence of the control strategy. In spring the daily electricity output can be increased from fixed pressure control with pressure retention valve by 39% by switching to variable pressure and variable condensation temperature. In winter, even greater differences between the control concepts can be determined. Here, the maximum power output represents an increase of a 65% in comparison to the value of the fixed pressure control with pressure retention valve. In comparison with the diurnal variations at full load in summer, the in this way optimized net power output is around 10% lower, although only 60% of the geothermal fluid mass flow are available. This makes it possible to produce an approximately constant electricity output over the year and to cover simultaneously the increasing demand for heat in winter.

4 CONCLUSION

The present contribution contains a detailed process analysis of a supercritical Organic Rankine Cycles for geothermal electricity generation at geothermal fluid temperatures of 150 °C using the example of the test facility MoNiKa. Based on a general thermodynamic optimization which included the choice of the working fluid propane, a dynamic model has been developed in Dymola using the library TIL. With this model the impact of varying cooling air conditions on the power requirement of the cooling fans as well as the part load behavior at three different control strategies have been investigated. It was found that the outdoor temperature has a significant impact on the power requirements of the cooler and thus also on the net performance of the process. While in the design case only 7.5% of the turbine power is need for the fans of the cooler, this proportion rises to over 30% at 40 °C ambient temperature at dry cooling mode. By injecting water in the hybrid mode the air can be cooled according to its relative humidity; in this way the decrease in the net power output can be reduced. A further possibility to counteract a reduction of the net power at high ambient temperatures is to adjust the condensation temperature on the ambient air temperature. This optimized cooler control also permits an increase in the net power output at low outside temperatures in relation to the design case. However, the turbo generator has to be designed to handle the higher pressure gradients and the increased power in this case. The simulations with reduced geothermal fluid mass flow showed a good part load behavior at sliding pressure control and at fixed pressure control with variable turbine speed. In contrary to fixed pressure control with pressure retention valve these control strategies allow a constant specific net power up to 50% load. However, it must be ensured in these cases that the components are suitable for the corresponding controls, i.e. the turbine can operate at variable speed and the heat exchanger allows both subcritical and supercritical flows.

REFERENCES

Dymola: **Version 2013 FD01**, *Dassault Systèmes* (1992-2012).

Ghasemi, H., Paci, M., Tizzanini, A., Mitsos, A.: Modeling and optimization of a binary geothermal power plant, *Energy,* **50**, (2013), 412-428.

IEA: Technology Roadmap Geothermal Heat and Power, International Energy Agency, Paris, France (2011)

Martin, H.: Pressure Drop and Heat Transfer in Plate Heat Exchangers, *VDI Heat Atlas*, **N6**, Second Edition, Springer, Berlin, Germany (2010), 1515-1522.

National Institute of Standards and Technology (NIST): NIST Standard Reference Database 23: Reference Fluid Thermodynamic and Transport Properties – REFPROP, **Version 9**, Gaithersburg, Colorado, USA (2010).

Numrich, R.,Müller, J.: Filmwise Condensation of Pure Vapors, *VDI Heat Atlas*, **J1**, Second Edition, Springer, Berlin, Germany (2010), 903-918.

Tchanche, B. F., Lambrinos, G., Frangoudakis, A., Papadakis, G.: Low-grade heat conversion into power using Organic Rankine Cycles – A review of various applications, *Renewable and Sustainable Energy Reviews,* **15**, (2011), Nr. 8, 3963-3979.

TIL: **Version 3.0.1**, *TLK-Thermo GmbH* (2012).

Vetter, C., Wiemer, H.-J., Kuhn, D.: Comparison of sub- and supercritical Organic Rankine Cycles for power generation from low-temperature/low-enthalpy geothermal wells, considering specific net power output and efficiency, *Applied Thermal Engineering*, **51**, (2013), Nr. 1-2, 871-879.

von Haaf, S., Steimle, F. (Ed), Stephan, K. (Ed.): Handbuch der Klimatechnik – Sechster Band / Teil B: Wärmeaustauscher: Wärmeübertragung in Kuftkühlern, Springer, Berlin, Germany (1988), 435-491.